Journal of
Water & Climate Change

 Journal of Water and Climate Change Vol 14 No 9, 3086 doi: 10.2166/wcc.2023.171

Integrated spatial and temporal variability of the system water use efficiency in a lower Baro River watershed, Ethiopia

Fiseha Befikadu [a,b,*], Amba Shetty [a] and Fekadu Fufa [c]

[a] Department of Water Resources and Ocean Engineering, National Institute of Technology Karnataka, Surathkal, Karnataka, India
[b] Department of Hydraulic and Water Resources Engineering, Mizan Tepi University, Mizan, Tepi, 260, Ethiopia
[c] Faculty of Civil and Environmental Engineering, Jimma Institute of Technology, Jimma University, Jimma, Oromia State, Ethiopia
*Corresponding author. E-mail: fishbefikadu@gmail.com

FB, 0000-0001-9165-3186; AS, 0000-0002-3633-5254; FF, 0000-0001-8974-0328

ABSTRACT

The Baro Akobo River is representative of lower Baro watersheds with lost soils. Under eight landscapes, the geospatial and temporal variability of system water use efficiency (sWUE) were examined in a total area of 20,325 km^2. This study used GIS, RS, Cropwat8.0, and EasyFit software. The anticipated irrigation requirement for the selected crop's driest five months of May, February, March, January, and April was 1, 0.9, 0.78, 0.78, and 0.34 l/s/h, respectively. The sub-catchment had maximum critical test values of $\sigma = 12.6$, $\mu = 11.9$, and $\gamma = 0$, while Sor Metu showed the smallest value of 0.80, 1.75, and -0.03. Across the watershed, the sWUE varies with runoff, with a coefficient of variation of 71%. The overall accuracy of the land cover change was 81%, the Landsat 8 images of the soil-adjusted vegetation index showed a maximum value of 0.87 and a minimum of -1.5. The normalized vegetation index ranged from a maximum of 0.58 to a minimum of -1. By 2050, the sWUE will be 10% lower temporally, but its spatial variability will be 25% higher. Therefore, soil infiltration and water storage improve, which decreases runoff and the water lost by ET and raises sWUE.

Key words: spatial and temporal variability, system water use efficiency, watershed

HIGHLIGHTS

- The study provides valuable information on possible future changes in system water use under a changing climate.
- A large amount of soil is eroded from the upstream and supplied to the lower watershed of Baro, Gambella, by the Baro Akobo River.
- Rainfall and temperature patterns over the watershed on hydrological variables and the change in land cover have an impact on the system for managing soil, water, and crops.

1. INTRODUCTION

A significant increase in water and land productivity is needed to feed the world's expanding population. Much can be achieved by irrigating more land and improving the operation and administration of current irrigation facilities. A key factor in boosting water use effectiveness and agricultural output is the use of irrigation and drainage systems in agriculture (Sun & Kulshreshtha 2023). A new product named LULC 2020 was released by the Environmental Systems Research Institute (ESRI) in June 2021. It was created by classifying Sentinel-2 satellite data at a 10-m resolution using artificial intelligence; information on land use, such as forestry, crops, water, and urban areas, is crucial and must be updated. The current generation of remote sensing (RS) technology enables high spatial and temporal resolution measurements of agricultural performance (Sanders & Masri 2016). Compared to WUE, sWUE considers runoff, better capturing the combined effects of soil management and climate on an agricultural system. Finding a balance between water needs for the environment and people is necessary for sustainable water resource management (Frederick *et al.* 2023). A target variable of interest and one or more predictor variables are connected empirically using statistical models (Dhillon 2023). The two main environmental elements that influence water resource planning and management at various scales are land cover (LC) and climate change (Malede *et al.* 2023). Ethiopia's maximum and minimum temperatures have risen by 0.37 and 0.28 °C each decade during the past few years, respectively (Chaemiso *et al.* 2016). The lower Baro navigation requirements should be satisfied by sustainable inland waterways without putting the well-being of riverine ecosystems at risk. Past studies have examined temporal changes in water use efficiency (WUE) for a single crop field resulting from variations in management (Wilson *et al.* 2022). The practical problem is how current crops and agricultural systems will be fair in terms of sustained productivity under different conditions as a result of rising water demands and weather variability. Current agricultural yield projections for the next few decades are not particularly optimistic if a business-as-usual strategy is maintained. Only a few studies take into account soil system WUE (sWUE) and how it fluctuates depending on the kind of soil and the management techniques used (Wilson *et al.* 2022). Estimates of sWUE variability will help us better understand how soil characteristics interact with management practices, which will help us make better crop selections and related decisions as the climate changes in the hydrological cycle.

2. LOWER BARO WATERSHED

The lower Baro watershed is located in the Southwestern part of the country between latitudes 8° 22′30″ N and longitudes 34° 20″36′ E, and covers an area of about 20,325 km^2. The eastern part of the basin consists of the hilly upland areas of a plateau and in the west near the borders of South Sudan. The basin is mountainous in altitude, which ranges below 500–3,000 m.a.s.l, with 50% of the area falling below 1,000 m.a.s.l and 42% between 1,000 and 2,000 m.a.s.l. The lower Baro watershed tributaries are shown in (Figure 1).

3. MATERIALS AND METHODS

In addition to satellite data, the Ethiopian National Meteorological Agency (ENMA) provided us with climatic information, such as rainfall and temperature from 1986 to 2018. In this study, eight tributaries of Baro were considered depending on the current status of the watershed, namely, the Alwero, Gilo Fugnido, Birbir Yubdo, Gog, Baro Gambella, Baro Itang, Gumero Gore, and Sor Metu. Moreover, the Esri 2020 LC map classes are computed by multiplying the number of pixels assigned to the class by the area of a pixel. Pixel counting is the name of this procedure; this approach has asymmetric classification errors despite being simple in the computing area; pixel counting skews the area's actual proportion. The lowlands have a sparse population, giving a favorable setting for the development of water resources. Aside from evapotranspiration (ET), runoff and drainage also affect the amount of water that is readily available in agricultural systems (Karimi & Bastiaanssen

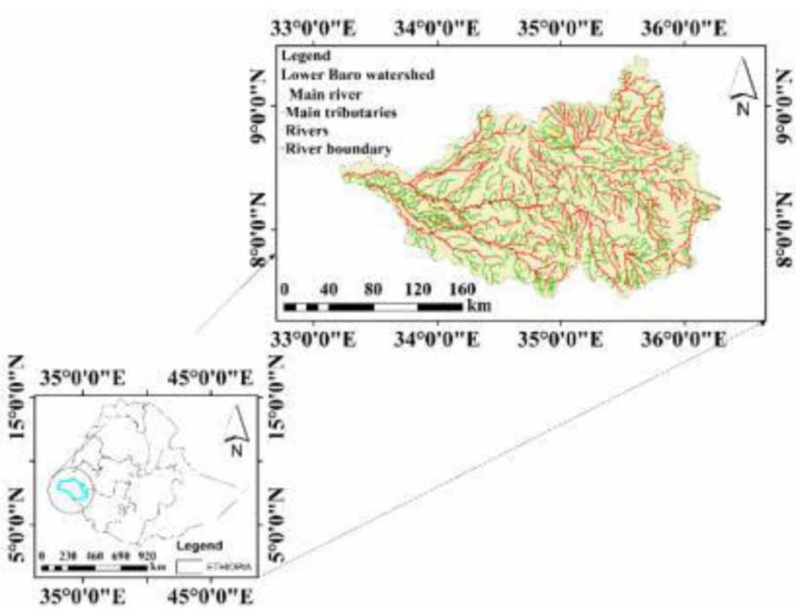

Figure 1 | Main tributaries of the lower Baro watershed.

2015). The systems WUE and sWUE take into account any additional water losses and are defined as shown in Equation (1).

$$\mathrm{sWUE} = \frac{\mathrm{Yield}}{\mathrm{ET} + \mathrm{Runoff} + \mathrm{Drainage}} \tag{1}$$

3.1. Land cover change at the watershed level

In this study, the sentinel-2 10 m resolution LC changes are applied. This is rather a simple process for water, dense forest, crops, constructed area, bare land, and clouds. Since they frequently appeared as a mixture of vegetation types and have varying appearances, the classes of scrub/shrub and flooded vegetation proved to be the most difficult (Dufera & Brijesh 2023). Land use has affected the water demand of crops grown in both irrigated and rainfed systems. Soil texture is one of the key elements affecting the soil's quality and suitability for agricultural production (Khalil 2017). The slope of infiltrating surface has the greatest effect on surface runoff production when the soil is closer to field capacity and even saturation. However, the hydro-geologically basin watershed is dominated by mining, and less water resource development has occurred so far (Worku Ayalew 2018; Halefom & Ulsido 2020). The slope, land suitability status, geology, and soil type maps of the lower Baro watershed are shown in Figure 2.

3.2. The goodness-of-fit tests

Information criterion methods are a measure of the relative goodness of fit and provide a means for the selection of a preferred distribution. They do not test how well the model fits are able to link models based on their goodness of fit. For this study, the EasyFit program by Mathware technologies was used to fit the statistical distribution. It includes several mathematical tools that can be used for the statistical analysis of extreme events. A large number of the statistical probability distributions, including all those discussed in these studies, are supported. In the Kolmogorov–Smirnov test, the maximum discrepancy is called the D-statistics (Dn), which is compared to the critical D-statistics (Yevjevich 1972). $f_n\ (x) = 1/n$ [number of observations) $< x$] $Dn =$ maximum $(Fn\ (x) - f(x))$. The critical D-statistic depends only on the sample size (n). Astafurov *et al.* (2017) provide a detailed table of critical distance values for a range of sample sizes. Since it was developed to confirm the data distribution, this test is regarded as a non-parametric test. In Anderson–Darling test statistics, the test

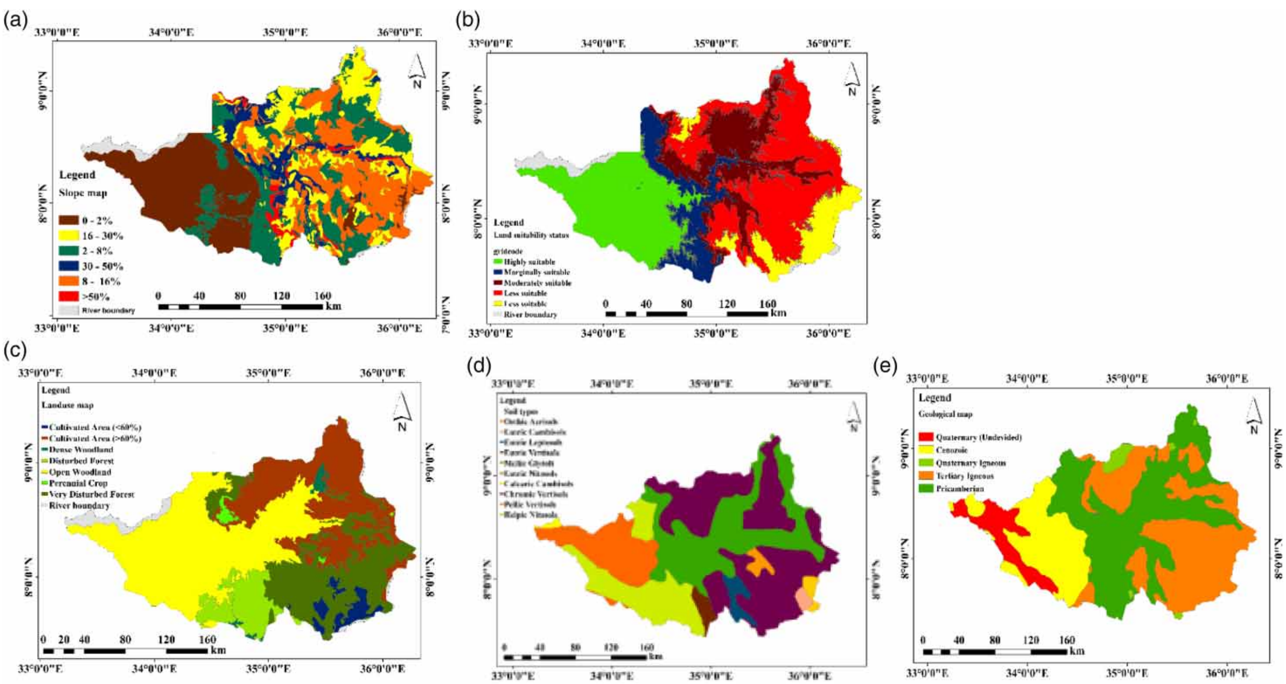

Figure 2 | (a) Slope map (2016–2019), (b) land suitability map, (c) land use map (2017–2020), (d) soil types map (FAO 2015), and (e) geological map (https://certmapper.cr.usgs.gov/data/apps/world-maps/).

assumes that there are no parameters to be estimated in the distribution being tested, in which case the test and its set of critical values are distribution-free as shown in Equation (2).

$$A^2 = \frac{1}{n}\sum_{t=1}^{n}(2i-1)[(\ln(f(xi)+\ln(1-f(x_{n-1}+1)] \quad (2)$$

where n is a sample size and i is an index of the dataset. The long-term rainy season rainfall and temperature trend variability (June–September) were examined using the eight stream gauging station data. Lastly, in the chi-squared goodness-of-fit test, a statistical test establishes whether or not a variable is likely to come from a given distribution.

3.3. Irrigation land suitability

In the land suitability map, the upstream and center portions of the area were found to be very suited for surface irrigation because of the short Euclidian distance from the water source, deep soil depth, flat slope, and high accessible surface water storage capacity. The SAVI is the soil-adjusted vegetation index, NIR is near-infrared stands for band 5, and RED is for band 4. L is typically equal to 1 in places with no green vegetation cover, 0.5 in areas with some green vegetation but not much, and 0 in areas with a lot of vegetation (which is equivalent to the Normalized Difference Vegetation Index (NDVI) method). The values produced by this index range from -1.0 to 1.0. This was often used in an arid region where vegetation cover was low and output values were between -1 and 1. In this study, the SAVI was quantified based on the data from USGS earth explorer from 03/30/2023 to 04/30/2023. The SAVI method is a vegetation index that attempts to minimize soil brightness influences using a soil brightness correction factor. The NDVI and SAVI equations are shown in Equations (3) and (4).

$$\text{SAVI} = \frac{(\text{NIR} - \text{RED})}{(\text{NIR} + \text{RED} + L)*(1 + L)} \quad (3)$$

$$\text{NDVI} = \frac{(\text{NIR} - \text{RED})}{(\text{NIR} + \text{RED})} \quad (4)$$

4. RESULTS AND DISCUSSION

Geospatial analysis was carried out to identify and classify diverse landscapes based on comparable hydrologic responses to quantify the geographical and temporal variability of WUE and sWUE in the lower Baro watershed tributaries. Ethiopia is a nation whose development is heavily dependent on agricultural products (Abdulahi *et al.* 2022). Irrigation, the biggest consumer of water resources, could support sustainability by implementing efficient water use techniques along with integrated agricultural methods intended to enhance the health of plants and the land. From 2016 to 2050, average temperatures during the growing season increased from 21 to 37.4 °C that were not a steady increase. Similarly, growing season precipitation totals for the lower Baro decreased by ~54 mm during this period, with the highest decrease after 2030. Spatially, values and patterns of growing season monthly temperature and precipitation were nearly identical, as the two classes overlap spatially. The monthly temperature and rainfall variations are shown in Figure 3.

As a result, in the lower Baro watershed, the CROPWAT8.0 indicates that the overall crop water demand for the four crop types, such as rice, sugarcane, maize, and vegetables, was 917.2 mm/decade throughout the entire growing season, and the total crop requires 7.02 l/s/h flows in each 1-ha area. In Ethiopian highlands in the Blue Nile Basin, a previous study mentioned that the majority of irrigation water demand occurred in all six irrigation nodes between the drier months of November and June, with little surface water management occurring between July and October (Yimere & Assefa 2022). The lowland Baro watershed projected values for rice, sugarcane, maize, and small vegetables in the chosen driest 5 months of May, February, March, January, and April were 1, 0.9, 0.78, 0.78, and 0.34 l/s/h, as shown in Table 1. When there is a lack of water, you must reconsider habits to maximize what is available.

4.1. Crop yields

For each crop, yields decreased from 2016 to 2050 following a similar stepped pattern as the growing season weather since yield is a function of both temperatures and precipitation. From 2014 to 2030, yields decreased by 9 and 18%, respectively, while maize yields increased by 5%. ET was the most significant water loss and moderately correlated with temperature and

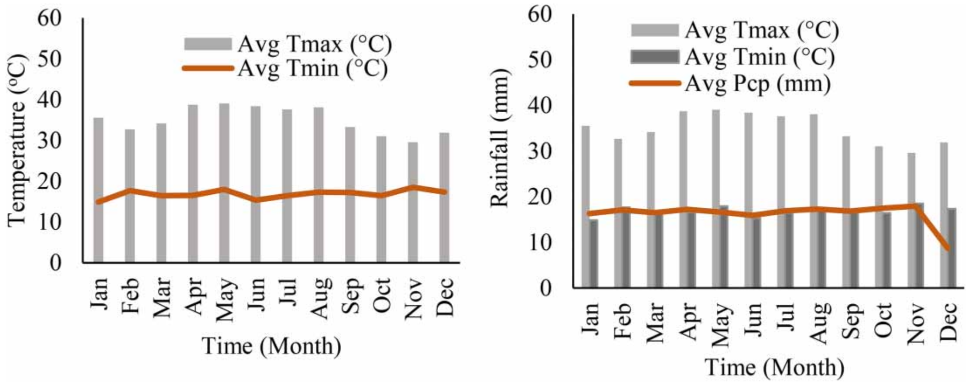

Figure 3 | Average monthly maximum and minimum temperature and rainfall from 1986 to 2018.

Table 1 | Irrigation scheme supply

Crop name	Jan	Feb	Mar	Apr	May	Jun	Jul	Aug	Sept	Oct	Nov	Dec
Rice deficit in mm	0	0	0	0	309	187.4	141.5	169.5	110.4	0	0	0
Sugarcane in mm	208.6	217.1	207.7	88.2	148.9	42	64.9	148.7	136.1	141.9	99.7	191.3
Maize in mm	0	0	0	0	0	41.3	105.4	171.1	96.7	7.3	0	0
Small vegetables	0	0	0	0	0	103.8	110.1	145.5	22.1	0	0	0
Net irrigation requirement												
Irrigation (mm/day)	0.5	0.6	0.5	0.2	2.7	2.2	2	2.8	1.6	0.4	0.3	0.4
Irrigation (mm/month)	16.7	17.4	16.6	7.1	83	66	62.7	86.2	46.6	11.9	8	15.3
Irrigation (l/s/h)	0.06	0.07	0.06	0.03	0.31	0.25	0.23	0.32	0.18	0.04	0.03	0.06
Irrigated area (% total area)	8	8	8	8	31	54	54	54	54	15	8	8
Irrigation requirement for the actual area (l//s/h)	0.78	0.9	0.78	0.34	1	0.47	0.43	0.6	0.33	0.3	0.38	0.71

precipitation. Irrigation, the biggest consumer of water resources, could support sustainability by implementing efficient water use techniques along with integrated agricultural methods intended to enhance the health of plants and the land. As a result, the Kolmogorov–Smirnov test, Anderson–Darling test statistics, and chi-squared goodness-of-fit test show significant changes in the rainfall and temperature in the distribution being tested. The test set of maximum critical values observed in the Baro Gambella sub-catchment shows that $\sigma = 12.6$, $\mu = 11.9$, and $\gamma = 0$, and the corresponding lowest observed result found in the Sor Metu sub-catchment shows that $\sigma = 0.80$, $\mu = 1.75$, and $\gamma = -0.03$. The lower Baro watershed is one of the tributaries of the White Nile in South Sudan, exhibiting high spatial and temporal rainfall variability (annual and seasonal). Rainfall tends to increase in the southern section of the watershed while tending to decrease in the northwest (Malede *et al.* 2022). This may be the result of topographical elements like climate change and rainfall and streamflow variability. Similar findings with Gebremicael *et al.* (2017) also stated that the monthly rainfall variation in the Tekeze Atbara basin is topographically determined. The comparison of WUE 1/3, 2/3, and 3/4 values with other published values was facilitated by multiple, recent meta-analyses. Measurements of WUE for maize range from 2 to 40 kg/ha/mm in 10 different countries with a large coefficient of variation, CV = 0.38 (Wilson *et al.* 2022). Rainfed rice, sugarcane, maize, and small vegetables in the lower Baro have WUE values ranging from 12 to 14 kg/ha/mm, while irrigated rice has lower WUE values from 2 to 3 kg/ha/mm due to the lower yields. Additionally, rotating maize with other crops decreased WUE from 25 to 4 kg/ha/mm and from 27 to 3 kg/ha/mm; increasing fertilizer rates raised WUE values from 9 to 23 kg/ha/mm across the Gambella region. The CV of the sWUE, which correlates rainfall and temperature with runoff, is 71% throughout the watershed. However, water savings brought on by irrigation technology are insufficient to support the increase in agriculture. A previous study proved that in East

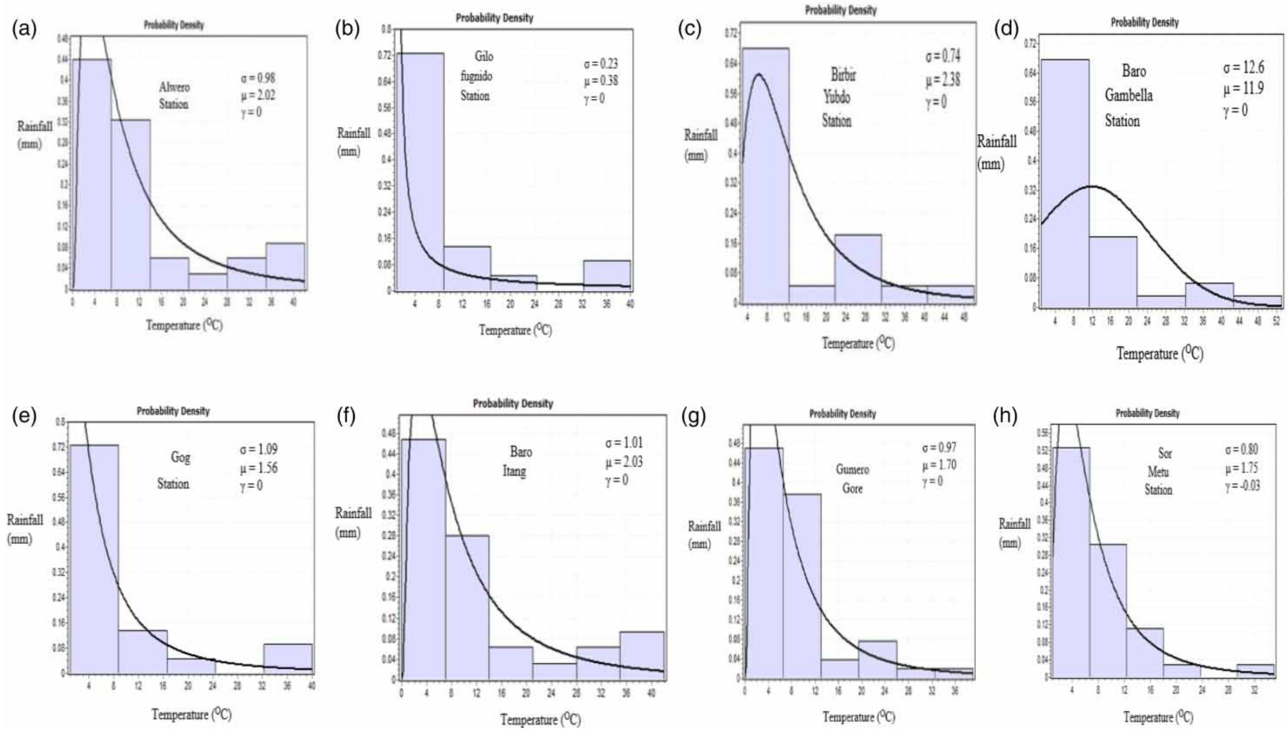

Figure 4 | Variability in temperature and rainfall over time lower Baro tributaries.

Africa, the annual flows and surface runoff are reduced by 131.9 and 255% when forest cover increases (Guzha *et al.* 2018). In this study, temperature and precipitation are two climatic factors that control yield gaps, along with crop water productivity. Numerous statistical probability distributions, such as those covered in these studies, have been supported (Mishra *et al.* 2013). One can quickly determine the chance of rainfall using the scale, shape, and other parameters (Mandal & Choudhury 2015). As a result, the variability in temperature and rainfall over time in eight stations is shown in Figure 4(a–h).

Annotators also accessed a similar high-resolution satellite picture through google maps and ground photography. Moreover, the Google Street view from the image's central point and the Sentinel-2 tile included the date and the center point's coordinates for every annotation. To balance efficiency and accuracy, each annotator was required to label at least 70% of a tile within 20–60 minutes, with some tiles allowed to be skipped. A previous study in the upper Baro proved that from 1986 to 2017 there is an increase in the flood frequency, peak flow, soil erosion, base flow, and annual mean discharge (Getu Engida *et al.* 2021). As a result of this study, the spatial extent of each LC type from the periods of 2017–2018, 2018–2019, 2019–2020, 2020–2021, 2021–2022, and 2022–2023 revealed that there was a decrease in the water body, cropland, and increase scrub/shrub land, trees, flooded vegetation, and bare ground over the past 5 years. The basin surface runoff potential was boosted from 37 to 49%, as we reviewed articles on the Ethiopian river basin (Dau *et al.* 2021). This is due to surface water variability having decreased as a result of land use (Alemayehu & Nigussie 2015; Giri *et al.* 2018). This scenario primarily happened because of the growing rate of population that triggered the intensification of demand for agricultural land, fuel wood, and as a source of economy. This, in turn, reduced other LC types of the study area, as shown in Figure 5(a–f).

Following best practices for accuracy assessment impact observatory adjusted the acreage estimate for each class using respective user accuracy as computed from the comparison to the validation set. The uncertainty surrounding the sample-based estimate of the area of deforested lower Baro was quantified as the confidence interval. However, information on the size of the classification mistakes was provided by the confusion matrix, which was used in the accuracy assessment, allowing the area estimator to be adjusted. Based on the analyses in this study, the overall accuracy of the LC change was 81% over the lower Baro watershed. The LULC 2020 (ESRI) with the addition of slope data and the GIS analysis findings on 281 test sites demonstrate a tremendous improvement in the overall accuracy of 84.34% (Kappa statistic 0.589). The

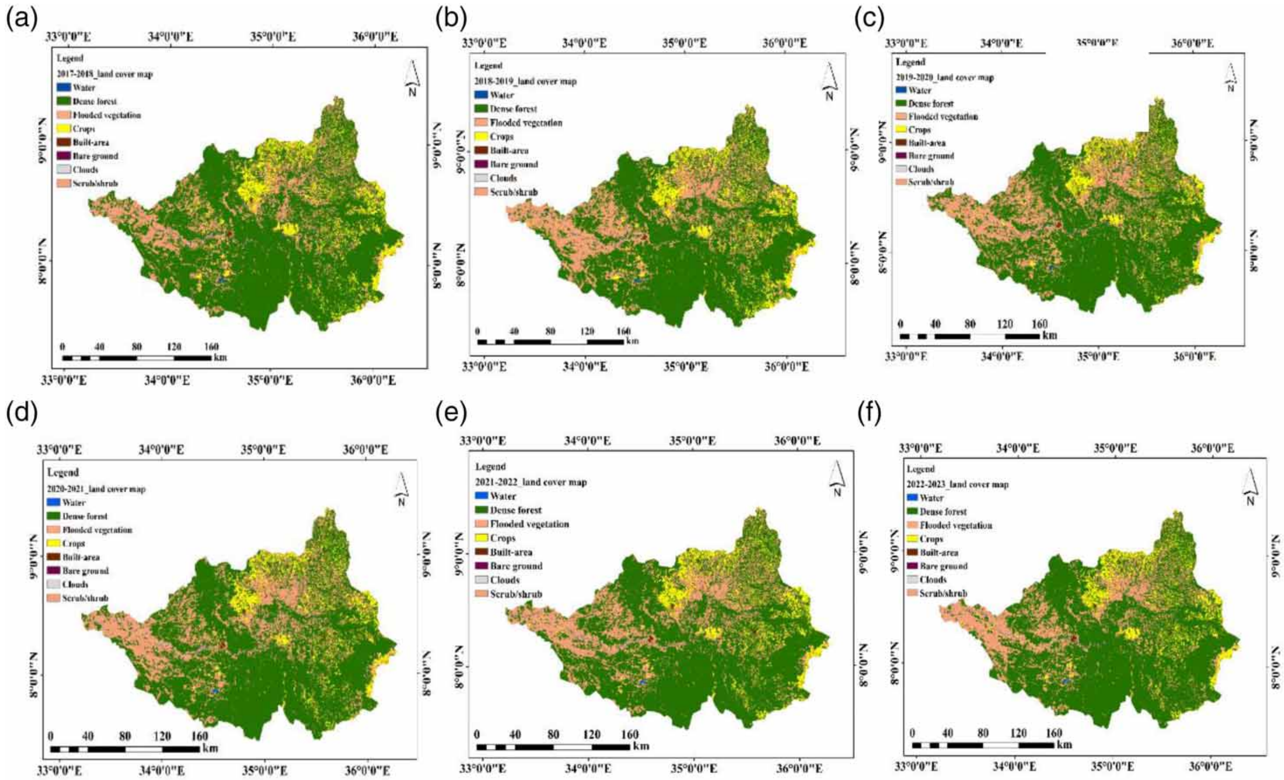

Figure 5 | Land cover map of the lower Baro watershed from 2017 to 2023.

accuracy of LULC 2020 (ESRI) data has significantly improved after integration with slope data, going from 79.72 to 84.34% overall, and can now be a useful option for land use statistics and inventory for management and planning. Free-of-charge land use and LC data are already classified by ESRI Inc. 2020 in moderate resolution as 10 m is the valuable source. Using this data for local land use management is challenging due to its limitations, as discussed above. This approach also allowed the impact of an observatory to produce a 95% confidence interval for each acreage estimate, providing users with a clearer picture of the accuracy and the total area for each class, as shown in Table 2.

Table 2 | Confusion matrix for the LC change

Land cover class	Water	Dense forest (trees)	Flooded vegetation	Crops	Built area	Bare ground	Scrub/ shrub	Row total	User accuracy	Commission error = 1 − user accuracy
Water	33	2.89	2.77	2.33	2.53	2.05	3.72	49.29	0.67	0.33
Dense forest (trees)	11.24	76	2.15	2.19	2.31	3.23	3.56	100.68	0.75	0.25
Flooded vegetation	8.23	2.89	79	2.12	1.78	2.12	2.16	98.3	0.80	0.20
Crops	3.23	2.78	2.65	76	1.97	3.18	2.27	92.08	0.83	0.17
Built area	3.69	2.61	2.78	1.98	73	2.48	2.15	88.69	0.82	0.18
Bare ground	2.45	2.23	1.31	1.08	2.26	67.2	2.96	79.49	0.85	0.15
Scrub/shrub	4.32	2.14	2.62	1.05	2.12	1.51	92	105.76	0.87	0.13
Column total	33.16	88.65	90.51	84.42	83.44	79.72	105.1	614.29	Overall accuracy	
Producer accuracy	1.00	0.86	0.87	0.90	0.87	0.84	0.88	Overall sum	81%	
Omission error = 1 − prod accuracy	0.00	0.14	0.13	0.10	0.13	0.16	0.12			

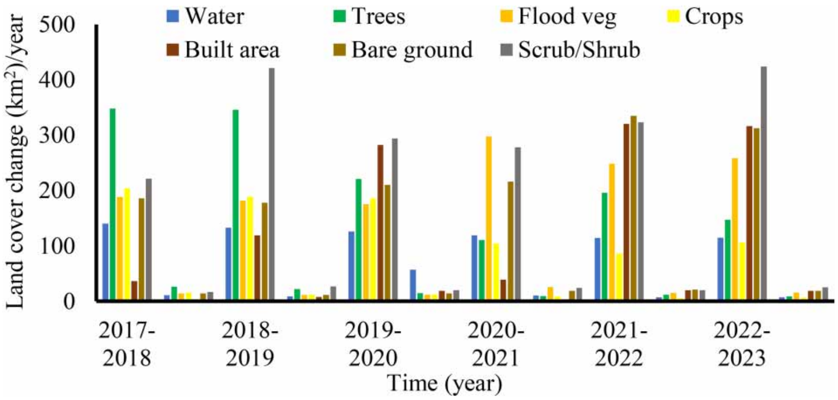

Figure 6 | Land cover change (km^2/yr) in the lower Baro watershed from 2017 to 2023.

In this study, the essential data and calculations are required to compile a thorough and exact report on the correctness of an LC map and area estimation result provided for the past 6 years from 2017 to 2023, as shown in Figure 6. LC change accuracy assessment has been completed, and an error matrix has been created, estimating the error-adjusted land change area and the confidence interval is not tricky but produces valuable information on change that may be very different from the results obtained solely from the map (Olofsson *et al.* 2013). Because LC is dynamic and is affected by several factors, they altered the hydrology of the basin watershed, making it crucial to assess their effects on various hydrological components. The effect of vegetation cover on enhancing basin capacity, preserving moisture, and increasing water production has been noted by researchers as something that cannot be ignored (Achugbu *et al.* 2022; Dufera & Brijesh 2023). This is because it can change how river catchments regulate their hydrological flow.

In particular for dry land areas of lower Baro, soil-adjusted vegetation indices have been created to offer better estimates of aboveground biomass. Because of their brightly reflecting soils and low vegetation cover, semi-arid rangelands frequently make it difficult to evaluate aboveground biomass using RS. The result of SAVI indicated a maximum value of 0.87 and a minimum value of −1.5, and the NDVI result shows a maximum value of 0.58 and a minimum value of −1. Previous studies indicated that the SAVI complements the NDVI when there is forest cover and vegetation in the LC, which accounts for 15% of the pixels (Vani & Mandla 2017). The NDVI and SAVI map are shown in Figure 7.

4.2. Comparison of WUE and sWUE with other studies

Recent meta-analyses from multiple sources have made it easier to compare WUE results with other published values. Measurements of WUE for maize range from 2 to 40 kg/ha/mm in 10 different countries with a significant CV of 0.38

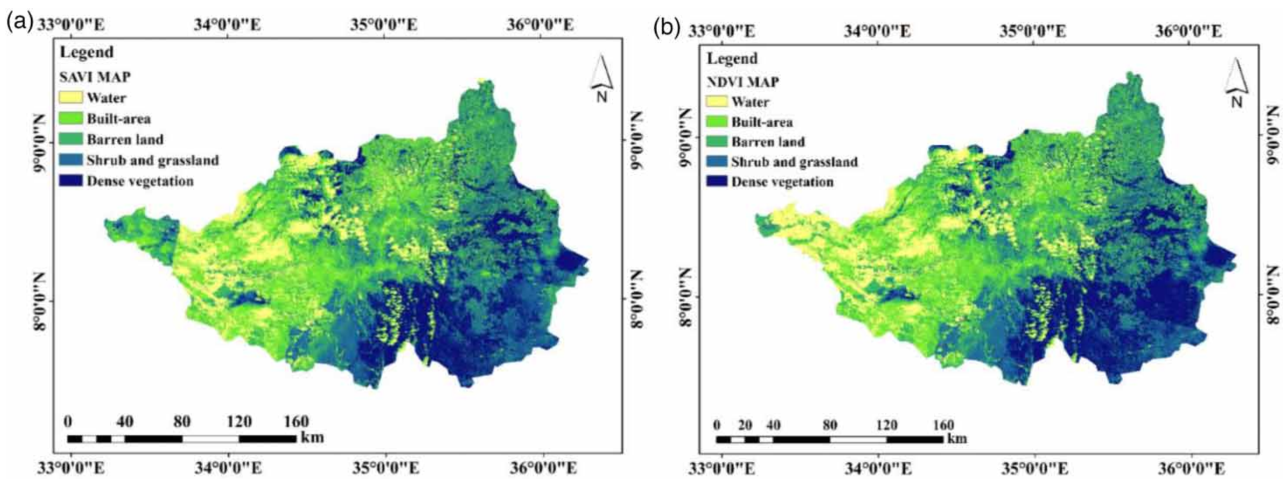

Figure 7 | (a) SAVI and (b) NDVI maps of lower Baro tributaries.

(Wilson *et al.* 2022). Rainfed rice, sugarcane, maize, and small vegetables in the lower Baro had WUE values ranging from 2 to 3 kg/ha/mm, while irrigated rice had lower WUE values from 2 to 3 kg/ha/mm due to the higher yields. Additionally, rotating maize with other crops increased WUE from 12–14 kg/ha/mm in Section 3.1 to 3–23 kg/ha/mm as increasing fertilizer rates raised WUE values from 9 to 26 kg/ha/mm across the Gambella region. In the Gambella region, rainfed maize has WUE values averaging 0.96–6.64 kg/ha/mm due to relatively high yields averaging 0.4 and 0.3 Mt in 1997–2017, respectively. Currently, increasing by 35%, which is near the maximum yield of 1.8 Mt, is seen in the lower Baro.

5. CONCLUSIONS

This study aimed at various aspects of geospatial investigation using GIS, RS, CROPWAT8.0, and EasyFit software. Eight distinct landscape types, including those with high-clay, high-organic matter soils, moderate slopes, and loss soils, without a layer at deep, were identified in the lower Baro watershed. The WUE gives a less realistic picture of how the LC changed from sentinel-2 with accuracy assessment using a confusion matrix, soil–water–crop management system functioning in agricultural systems than the sWUE index, which takes runoff and drainage into account in addition to ET. The novelty of this study is that it investigates the significance of considering spatial variability in landscape features (i.e., various soil-slope combinations) and its impact on WUE and sWUE within a representative of the watershed. Short-term climatic droughts are projected to arise from a 34 °C increase in the growing season, affecting the water consumed in the watershed. The CROPWAT8.0 shows that the total crop water demand for the four crop types, rice, sugarcane, maize, and vegetables, was 917.2 mm/decade over the full growing season, and the total crop demand of 7.02 l/s/h flows in each 1-ha area. The temperature between 2016 and 2050 is a commensurate drop in October precipitation totals. Maize and small vegetable yields over lower Baro have significant yield declines of 20 and 35%, respectively. The rice yields have seen a 5% decline; as a result, sWUE values have dropped. From the moisture absorption perspective, minimizing the ET transpiration stream is very beneficial. In addition, Landsat 8 showing how the NDVI and SAVI were affected by soil moisture and meteorological factors was analyzed. The timing of irrigation activities is crucial to determine which management measures would mitigate the effects of a more variable climate on sWUE. These variables might affect the unpredictability of water usage and storage in a watershed at various spatial scales. These practices enhance infiltration and water storage in the soil, which, in turn, reduces runoff and standing water lost through ET and increases sWUE. Our findings provide a critical baseline for future management planning of sustainable surface water resource consumption.

ACKNOWLEDGEMENTS

The authors acknowledge the Ethiopian Ministry of Water Resources, Irrigation, and Energy for providing basins shapefiles and the Ethiopian National Meteorological Agency for the climatic data. The LC dataset was produced by the impact observatory for Esri. This dataset is available under a creative commons BY-4.0 license and a copy of or works on this dataset requires the following attributions. This dataset is based on the dataset produced for the dynamic world project by the National Geographic Society in partnership with Google and the World Resource Institutes.

DATA AVAILABILITY STATEMENT

All relevant data are included in the paper or its Supplementary Information.

CONFLICT OF INTEREST

The authors declare there is no conflict.

REFERENCES

Abdulahi, S. D., Abate, B., Harka, A. E. & Husen, S. B. 2022 Response of climate change impact on stream flow: the case of the Upper Awash. *Water and Climate Change* **13** (2), 607–628. https://doi.org/10.2166/wcc.2021.251.

Achugbu, I. C., Olufayo, A. A., Balogun, I. A., Dudhia, J., McAllister, M., Adefisan, E. A. & Naabil, E. 2022 Potential effects of land use land cover change on streamflow over the Sokoto Rima River Basin. *Heliyon* **8** (e09779), 7. https://doi.org/10.1016/j.heliyon.2022.e09779.

Alemayehu, K. & Nigussie, H. 2015 Land use/cover change and its implication on soil erosion: a case study of Baro River Basin in South Western Ethiopia. *Journal of Environment and Earth Science* **5** (8), 53–58.

Astafurov, V. G., Kur'yanovich, K. V. & Skorokhodov, A. V. 2017 A statistical model for describing the texture of cloud cover images from satellite data. *Russian Meteorology and Hydrology* **42** (4), 248–257. https://doi.org/10.3103/S1068373917040057.

Chaemiso, S. E., Abebe, A. & Pingale, S. M. 2016 Assessment of the impact of climate change on surface hydrological processes using SWAT: a case study of Omo-Gibe river basin, Ethiopia. *Modeling Earth Systems and Environment* **2** (4), 1–15. https://doi.org/10.1007/s40808-016-0257-9.

Dau, Q. V., Kuntiyawichai, K. & Adeloye, A. J. 2021 Future changes in water availability due to climate change projections for Huong Basin, Vietnam. *Environmental Processes* **8** (1), 77–98. https://doi.org/10.1007/s40710-020-00475-y.

Dhillon, M. S. 2023 Seasonal precipitation forecasting for water management in the Kosi Basin, India using large-scale climate predictors. *Journal of Water and Climate Change* **00** (0), 1–13. https://doi.org/10.2166/wcc.2023.479.

Dufera, T. & Brijesh, T. 2023 Assessment of land use/land cover change impact on streamflow: a case study over upper Guder Catchment, Ethiopia. *Sustainable Water Resources Management* **9**, 6.

FAO 2015 *World Reference Base for Soil Resources 2014. International Soil Classification System for Naming Soils and Creating Legends for Soil Maps*. Update 2015. FAO, Rome.

Frederick, J., Michael, D. T., Promentilla, A. B. & Smarandache, F. 2023 Addressing uncertainties in planning sustainable systems through multi-criteria decision analysis (MCDA). *Process Integration and Optimization for Sustainability* **6** (Smarandache 2006), 3–4. https://doi.org/10.1007/s41660-023-00317-y.

Gebremicael, T. G., Mohamed, Y. A., Zaag, P. V. & Hagos, E. Y. 2017 Temporal and spatial changes of rainfall and streamflow in the Upper Tekezē-Atbara river basin, Ethiopia. *Hydrology and Earth System Sciences* **21** (4), 2127–2142.

Getu Engida, T., Nigussie, T. A., Aneseyee, A. B. & Barnabas, J. 2021 Land use/land cover change impact on hydrological process in the Upper Baro Basin, Ethiopia. *Applied and Environmental Soil Science* **2021**, 15. https://doi.org/10.1155/2021/6617541.

Giri, S., Arbab, N. N. & Lathrop, R. G. 2018 Water security assessment of current and future scenarios through an integrated modeling framework in the Neshanic River Watershed. *Journal of Hydrology* **563** (May), 1025–1041. https://doi.org/10.1016/j.jhydrol.2018.05.046.

Guzha, A. C., Rufino, M. C., Okoth, S., Jacobs, S. & Nóbrega, R. L. B. 2018 Impacts of land use and land cover change on surface runoff, discharge, and low flows: evidence from East Africa. *Journal of Hydrology: Regional Studies* **15** (November 2017), 49–67. https://doi.org/10.1016/j.ejrh.2017.11.005.

Halefom, A. & Ulsido, M. D. 2020 Land Suitability Assessment for Surface Irrigation of Baro Akobo River Basin Land Suitability Assessment for Surface Irrigation of Baro Akobo River Basin. In *1st International Conference on Engineering and Technology(ICET)*, November, pp. 154–164.

Karimi, P. & Bastiaanssen, W. G. M. 2015 Spatial evapotranspiration, rainfall, and land use data in water accounting – part 1: review of the accuracy of the remote sensing data. *Hydrology and Earth System Sciences* **19** (1), 507–532. https://doi.org/10.5194/hess-19-507-2015.

Khalil, R. 2017 Determination of potential runoff coefficient using GIS and remote sensing. *Journal of Geographic Information System* **09** (06), 752–762. https://doi.org/10.4236/jgis.2017.96046.

Malede, D. A., Agumassie, T. A., Kosgei, J. R., Linh, N. T. T. & Andualem, T. G. 2022 Analysis of rainfall and streamflow trend and variability over Birr River watershed, Abbay basin, Ethiopia. *Environmental Challenges* **7**, 100528. https://doi.org/10.1016/j.envc.2022.100528.

Malede, D. A., Alamirew, T. & Andualem, T. G. 2023 Integrated and individual impacts of land use land cover and climate changes on hydrological flows over Birr River. *Water* **15** (1), 66. https://doi.org/10.3390/w15010166.

Mandal, S. & Choudhury, B. U. 2015 Estimation and prediction of maximum daily rainfall at Sagar Island using best-fit probability models. *Theoretical and Applied Climatology* **121** (1–2), 87–97. https://doi.org/10.1007/s00704-014-1212-1.

Mishra, P. K., Khare, D., Mondal, A., Kundu, S. & Shukla, R. 2013 Statistical and probability analysis of rainfall for crop planning in a canal command. *Agronomy for Sustainable Development* **1** (1), 95–102.

Olofsson, P., Foody, G. M., Stehman, S. V. & Woodcock, C. E. 2013 Making better use of accuracy data in land change studies: estimating accuracy and area and quantifying uncertainty using stratified estimation. *Remote Sensing of Environment* **129** (122–131), 10. https://doi.org/10.1016/j.rse.2012.10.031.

Sanders, K. T. & Masri, S. F. 2016 The energy-water agriculture nexus: the past, present and future of holistic resource management via remote sensing technologies. *Journal of Cleaner Production* **117** (73–88), 16. https://doi.org/10.1016/j.jclepro.2016.01.034.

Sun, R. & Kulshreshtha, S. N. 2023 Corrected proof enhancing environmental sustainability in eastern Canada's corn agroecosystem with controlled drainage and subsurface irrigation. *Journal of Water and Climate Change* **00** (0), 1–12. https://doi.org/10.2166/wcc.2023.509.

Vani, V. & Mandla, V. R. 2017 Comparative study of NDVI and SAVI vegetation indices in Anantapur district semi-arid areas. *International Journal of Civil Engineering and Technology* **8** (4), 559–566.

Wilson, C. G., Papanicolaou, A. N., Abban, B. K. B., Freudenberg, V. B., Ghaneeizad, S. M., Giannopoulos, C. P. & Hilafu, H. T. 2022 Comparing spatial and temporal variability of the system water use efficiency in a Lower Mississippi river watershed. *Journal of Hydrology: Regional Studies* **42**, 101141.

Worku Ayalew, D. 2018 Theoretical and empirical review of Ethiopian water resource potentials, challenges, and future development opportunities. *International Journal of Waste Resources* **08** (04). https://doi.org/10.4172/2252-5211.1000353.

Yevjevich, V. 1972 *Structural Analysis of Hydrologic Time Series*. Colorado State University, Fort Collins, CO, Hydrology Paper no. 56 (pp. 59).

Yimere, A. & Assefa, E. 2022 Current and future irrigation water requirement and potential in the Abbay River Basin, Ethiopia. *Air, Soil and Water Research* **15** (1–15), 14.

First received 26 March 2023; accepted in revised form 7 August 2023. Available online 18 August 2023